ARTICLE
Journal of Cellular Biochemistry 115:531–539 (2014)

Journal of Cellular Biochemistry

Transplantation of iPSc Ameliorates Neural Remodeling and Reduces Ventricular Arrhythmias in a Post-Infarcted Swine Model

Fengxiang Zhang,[1] Guixian Song,[1] Xiaorong Li,[1] Weijuan Gu,[1] Yahui Shen,[2] Minglong Chen,[1] Bing Yang,[1] Lingmei Qian,[1]* and Kejiang Cao[1]**

[1]*Department of Cardiology, The First Affiliated Hospital of Nanjing Medical University, Nanjing 210029, People's Republic of China*

[2]*Department of Cardiology, Nanjing Maternity and Child Health Care Hospital Affiliated to Nanjing Medical University, Nanjing 210029, People's Republic of China*

ABSTRACT

Neural remodeling after myocardial infarction (MI) may cause malignant ventricular arrhythmia, which is the main cause of sudden cardiac death following MI. Herein, we aimed to examine whether induced pluripotent stem cells (iPSc) transplantation can ameliorate neural remodeling and reduce ventricular arrhythmias (VA) in a post-infarcted swine model. Left anterior descending coronary arteries were balloon-occluded to generate MI. Animals were then divided into Sham, PBS control, and iPS groups. Dynamic electrocardiography programmed electric stimulation were performed to evaluate VA. The spatial distribution of vascularization, Cx43 and autonomic nerve regeneration were evaluated by immunofluorescence staining. Associated protein expression was detected by Western blotting. Likewise, we measured the enzymatic activities of superoxide dismutase and content of malondialdehyde. Six weeks later, the number of blood vessels increased significantly in the iPSc group. The expression of vascular endothelial growth factor and connexin 43 in the iPS group was significantly higher than the PBS group; however, the levels of nerve growth factor and tyrosine hydroxylase were lower. The oxidative stress was ameliorated by iPSc transplantation. Moreover, the number of sympathetic nerves in the iPSc group was reduced, while the parasympathetic nerve fibers had no obvious change. The transplantation of iPSc also significantly decreased the low-/high-frequency ratio and arrhythmia score of programmed electric stimulation-induced VA. In conclusion, iPSc intramyocardial transplantation reduces vulnerability to VAs, and the mechanism was related to the remodeling amelioration of autonomic nerves and gap junctions. Moreover, possible mechanisms of iPSc transplantation in improving neural remodeling may be related to attenuated oxidative stress and inflammatory response. J. Cell. Biochem. 115: 531–539, 2014. © 2013 Wiley Periodicals, Inc.

KEY WORDS: MYOCARDIAL INFARCTION; VENTRICULAR ARRHYTHMIA; INDUCED PLURIPOTENT STEM CELL; TRANSPLANTATION; NEURAL REMODELING

Fatal ventricular arrhythmia (VA) is a common complication after acute myocardial infarction (MI) and accounts for nearly 50% of sudden cardiac deaths among patients surviving MI [Huikuri et al., 2001]. Despite the vastness of this problem, both the identification of factors contributing to VA and the development of safe and effective anti-arrhythmic agents remain elusive.

Hearts are innervated by both sympathetic and parasympathetic nerves. These two types of nerves compose a complex nerve network to regulate heart rhythm and myocardial contraction strength. The myocardium, blood vessels, and autonomic nerves undergo a process of damage, regeneration and reconstruction after MI. Cao et al. [2000] demonstrated that there is an association between the history of

Fengxiang Zhang, Guixian Song, and Xiaorong Li contributed equally to this study.
Conflict of Interest: No conflict of interest exists in the submission of this manuscript.

Grant sponsor: National Natural Science Foundation of China; Grant numbers: 81170160, 30871077, 30800464; Grant sponsor: The Program for Development of Innovative Research Team in the First Affiliated Hospital of Nanjing Medical University; Grant number: IRT-004; Grant sponsor: The Six Peak Talents Foundation of Jiangsu Province; Grant number: 2011-WS-071.

*Correspondence to: Dr. Lingmei Qian, Department of Cardiology, The First Affiliated Hospital of Nanjing Medical University, Nanjing 210029, People's Republic of China. E-mail: lmqian@njmu.edu.cn
**Correspondence to: Kejiang Cao, Department of Cardiology, The First Affiliated Hospital of Nanjing Medical University, Nanjing 210029, People's Republic of China. E-mail: kejiangcao@163.com

Manuscript Received: 9 July 2013; Manuscript Accepted: 26 September 2013
Accepted manuscript online in Wiley Online Library (wileyonlinelibrary.com): 5 October 2013
DOI 10.1002/jcb.24687 • © 2013 Wiley Periodicals, Inc.

spontaneous VA and increased density of sympathetic nerves. This correlation is further supported by the finding that attenuated sympathetic reinnervation is associated with less frequent VA [Liu et al., 2003; Lee et al., 2007]. The latter study uncovered a strong correlation between abnormally increased nerve sprouting and the occurrence of VA and sudden cardiac death. Subsequently, Billman [2009] showed that subnormal cardiac parasympathetic regulation coupled with elevated cardiac sympathetic activation may allow for the formation of malignant VA. These results suggest that future development of anti-arrhythmic interventions should target not only electrical remodeling and myocardial remodeling, but also neural remodeling after MI.

Various therapeutic efforts, such as anti-arrhythmic drugs, which have had little effect, and the implantable cardioverter defibrillator, which is too expensive for standard patient use, have been used to prevent potentially fatal VA following infarction. Recently, novel ESC-like pluripotent stem cells, known as "induced pluripotent stem cells" (iPSc), were generated from mice by transducing mouse embryonic or adult dermal fibroblasts with retroviruses encoding Oct3/4, Sox2, c-Myc, and Klf4 [Takahashi and Yamanaka, 2006]. In theory, iPSc are capable of differentiating into a variety of cell types as needed, including cardiovascular cells [Narazaki et al., 2008; Seki et al., 2010]. Because of the simplicity and high efficiency of generating patient-specific pluripotent stem cells, iPSc were considered to be the most promising candidate for cardiac regeneration treatments. However, the effect of iPSc transplantation on nerve regeneration and VA after MI has not been explored.

In the present study, we injected undifferentiated iPSc into injured myocardium to test the hypothesis that this novel cell-based therapy can ameliorate cardiac autonomic neural remodeling and thus exert an anti-arrhythmic effect.

MATERIALS AND METHODS

ANIMALS

Two-month-old suzhong swine (25 ± 5 kg) were obtained from the Nanjing Academy of Agricultural Sciences. All experimental procedures were performed in accordance with the Guide for the Care and Use of Laboratory Animals published by the US National Institutes of Health and was approved by the Experimental Animal Ethics Committee of Nanjing Medical University, China.

CELL CULTURE AND PREPARATION

iPS cells were kindly provided by professor Lei Xiao (Shanghai Institutes for Biological Sciences, Chinese Academy of Sciences, Shanghai, China). This porcine iPSc line was derived from primary ear fibroblasts or primary bone marrow cells of 10-week-old Danish Landrace pigs, and was generated by drug-inducible expression of a combination of six genes (Oct4, Sox2, Nanog, Lin28, c-Myc, and Klf4). Cell culture and iPSc properties were described by Wu et al. [2009]. iPS cells were transduced with adenovirus expressing the enhanced green fluorescent protein (GFP) reporter gene and cultured on irradiated mouse embryonic fibroblasts (Fig. S1A,B).

ESTABLISHMENT OF AN ACUTE MYOCARDIAL INFARCTION MODEL

The MI model was established as described previously described [Yang et al., 2008]. Following the successful establishment of the model (Fig. S1C,D), mini-swine ($n = 18$) were randomly allocated to three groups as follows:

- Sham group ($n = 6$); Coronary angiography but without Left anterior descending (LAD) occlusion;
- PBS group ($n = 6$); LAD occlusion followed by phosphate buffer solution (PBS) injection after a week;
- iPS group ($n = 6$); LAD occlusion followed by iPSc transplantation after a week.

iPSc TRANSPLANTATION

One week after MI induction, an open-chest operation was carried out for cell transplantation (Fig. S1E). The infarcted region was identified by color change from bright red to dark blue and abnormal wall motion. iPSc (2×10^7) or an equal placebo volume of PBS was injected by sterile microinjection at ten sites both in the infarction zone (IZ) and border zone (BZ) as determined by direct visualization (Fig. S1F). The needle was advanced 5 mm into the myocardium. Haemostasis was performed and the chest was closed in layers. Postoperatively, penicillin G benzathine (30,000 U/day) was administered intravenously for 3 days. In addition, cyclosporine and methylprednisolone were injected intramuscularly for 2 weeks in the iPS and PBS group as previously described [Zeng et al., 2007], which helps to alleviate the non-specific immune response and the acute inflammatory reactions.

TWO-HOUR DYNAMIC ELECTROCARDIOGRAPHY

Six weeks later, the pigs received anesthesia and were stabilized in an operation table. Two-hour dynamic electrocardiography was obtained using a dynamic digital ECG recorder (General Electric Company). The data were recorded by a blinded operator, using ECG Auto 1.5.7 software (EMKA Technologies). A random sample of a 5-min ECG recording exclusive of non-sinus beats was selected for the analysis of heart rate variability as described by other investigators [Kruger et al., 1997]. The peak of the R spike served as a reference point for the temporal location of the R wave. In the time domain, the mean gap between beat-to-beat intervals (the NN-interval, ms), the SD of the NN-interval, and the coefficient of variance (100 SD of NN-interval/mean NN-interval) were calculated. In the frequency domain, two regions of interest were defined: low-frequency (LF) ($0.5\ \text{Hz} < \text{LF} < 0.8\ \text{Hz}$) and high-frequency (HF) ($0.8\ \text{Hz} < \text{HF} < 4.5\ \text{Hz}$) bands, and the LF/HF ratio was calculated.

IN VIVO ELECTROPHYSIOLOGICAL STUDY

After completion of the 2-h dynamic electrocardiography, a 6F electrophysiology electrode catheter was introduced in an intravenous sheath pipe into the apical right ventricle, and then programmed electrical stimulation was performed. Arrhythmias were induced using an electric Bloom stimulator (Chengdu Electronic Machine Company). To induce VA, eight paced beats at a cycle length of 120 ms (S1) were applied, followed by one to three extra stimuli (S2, S3, and S4) at shorter coupling intervals. The end point of ventricular pacing was the induction of VA. VA, including ventricular tachycardia and ventricular fibrillation, were considered non-

sustained when they lasted $\leq$15 beats and sustained when they lasted >15 beats. An arrhythmia scoring system was modified as previously described [Kang et al., 2009]. The experimental protocols were typically completed within 10 min.

ANIMAL SACRIFICE AND SPECIMEN PROCESS

At the end point of each animal, the heart was removed and sectioned from the occlusion location of the apex into five transverse slices in a plane parallel to the atrioventricular groove. The left ventricular (LV) sections were divided into three portions as described by Zhang et al. [2007]: the infarct zone, defined as a myocardial region devoid of myocytes; the peri-infarct region, the region 2 cm away from the infarct zone; and the distant region, the region 5 cm away from the infarction. Individual respective tissues were isolated and preserved in liquid nitrogen at −196°C for future use.

ANTIOXIDANT ENZYME ACTIVITIES AND LIPID PEROXIDATION

The tissues of BZ in MI hearts and control myocardial tissues were collected at defined endpoints and analyzed for determination of the oxidative stress level. The enzymatic activities of superoxide dismutase (SOD) were measured through the xanthine-oxidation method according to the manufacturer's instructions (Jiancheng Institute, Nanjing, China) as previously described [Ho et al., 1997]. In shoring, the measurement was performed in the presence of 10 mM KCN to eliminate the activity of tissue cytochrome c oxidase. To distinguish the contribution of copper-zinc SOD and manganese SOD to the total SOD activity, the same measurement was also repeated in the presence of 1 mM KCN to inhibit the activity of copper-zinc SOD. One unit of SOD activity is defined as the enzyme activity needed to inhibit 50% cytochrome c reduction. The myocardial content of malondialdehyde, a secondary product of lipid peroxidation, was determined by measuring levels of thiobarbituric acid-reactive substance (Jiancheng Institute) as previously described [Kikugawa et al., 1992].

WESTERN BLOT ANALYSIS

At 6 weeks after MI, pulverized frozen samples from the BZ of infarction were analyzed by quantitative immunoblotting using antibodies against vascular endothelial growth factor (VEGF) (1:1,000; SAB2502119; Sigma–Aldrich), nerve growth factor (NGF) (1:500; ab6199; Abcam), antityrosine hydroxylase (TH) (1:400; ab6211; Abcam) and connexin 43 (Cx43) (1:500; C6219; Sigma–Aldrich). The protein concentrations of the samples were determined by the BCA method. Proteins (50 μg) were resolved by 14% sodium dodecyl sulfate–polyacrylamide gel electrophoresis (SDS–PAGE) and transferred to a PVDF membrane. Primary antibody was added after blocking the membrane and incubated with the membrane overnight at 4°C. The housekeeping protein GAPDH (1:5,000; ab8245; Abcam) was used as an internal standard. Horseradish peroxidase-linked secondary antibodies (Zhongshan Golden Bridge) were used, and proteins were visualized by an ECL kit. The bands were then exposed to radiography film, followed with densitometric quantification by imageJ software analysis.

IMMUNOFLUORESCENCE ANALYSIS

The transplanted iPSc had been engineered to express GFP; thus, the survival and differentiation of transplanted iPSc were evaluated by staining for the expression of GFP, actin, and vWF. The distribution of the GFP-positive cells suggested the survival of transplanted cells. In addition, the spatial distribution of vascularization, Cx43 and autonomic nerve regeneration were also evaluated by immunofluorescence staining. The following antibodies were used for these experiments: mouse anti-α-smooth muscle cell actin (α-SMA) (1:100, ab5694; Abcam), rabbit anti-Cx43 (1:1,000; C6219; Sigma–Aldrich) rabbit anti-von Willebrand factor (vWF) (1:400; ab68545; Abcam), mouse anti-TH (TH) (1:400; ab6211; Abcam), and acetylcholinesterase (Ache) (1:400; ab2803; Abcam). Samples from the BZ or a corresponding zone of the Sham group taken from liquid nitrogen were embedded immediately into an optimal cutting temperature compound (Miles-Bayer) and cut into 5-μm sections. The slices were rinsed and then incubated with the primary antibody at 4°C overnight. The next day, the slices were rinsed five times and incubated prior to the addition of secondary antibody.

The slices were coded so that the investigator was blinded to the identification of the pig sections. Vessel density was expressed as the number of SMA positives per square millimeter. Under a fluorescence microscope, the vessel density counts in each group were averaged from 30 fields (six slices and five areas in each slice). The nerve density was measured by computerized planimetry (Image ProPlus, Media Cybernetics, SilverSpring, MD) as described previously [Lee et al., 2004]. Five fields at 400× magnification were randomly selected, and the density was expressed as an average ($\mu m^2/mm^2$). All the Cx43 images were recorded using the same settings and the pixel intensities, five fields at 400× magnification per slice were randomly selected and analyzed using Image ProPlus.

STATISTICAL ANALYSIS

Continuous variables were expressed as mean ± SD and compared by Student's *t*-test or one-way analysis of variance (ANOVA) test, Kruscal–Wallis H tests, and Mann–Whitney U tests were used when the data were not met the normal distribution criteria or homogeneity of variance. Categorical variables were presented as percentage and compared by chi-square test unless otherwise indicated. Statistical analyses were performed using SPSS software (SPSS, Inc). A value of $P < 0.05$ was considered significant.

RESULTS

GENERAL CHARACTERISTICS OF MI

The ECG showed clear ST segment elevation in leads V1–V3 after complete occlusion of the distal LAD (Fig. S2A). Some pigs experienced ventricular fibrillation during the model creation (Fig. S2B). At 6 weeks post-operation, ventriculography was performed to identify ventricular aneurysm formation in the infarcted groups (Fig. S2C). In addition, TTC staining was performed to identify the infarcted myocardium (Fig. S2D).

IDENTIFICATION OF SURVIVING iPSc

At 6 weeks post-cell transplantation, fluorescent immunostaining for GFP was carried out to identify the transplanted cells in the heart. Frozen sections showed GFP-positive cells distributed in all regions in the iPS group, whereas most transplanted cells were found in the border zone. The distribution of the GFP-positive cells suggested the

survival of transplanted cells. In many regions, the GFP-positive spots were coincident with the red fluorescence spots of the vWF antibody (Fig. 1A), indicating that labeled iPSc were actively differentiated into vascular endothelial cells in vivo although they did not actively survive as myoblasts or smooth muscle cells (Fig. 1B). In contrast, sections from the control and Sham groups showed no evidence of red and green fluorescence.

REDUCED OXIDATIVE STRESS IN THE HEART FOLLOWING iPSc TREATMENT

At the end point, SOD activity in post-infarction myocardium was significantly higher in the PBS and iPS groups than in the Sham group (109.5 ± 12.2, 98.8 ± 11.3, and 81.4 ± 7.8 U/mg protein, respectively, $P < 0.05$); however, compared to the PBS group, SOD activity in the iPSc group was significantly lower (Fig. 2A), indicating that iPSc treatment enhanced the ability to scavenge free radicals in post-infarcted myocardium. In contrast, the malondialdehyde content of the myocardium was lower in the iPSc group than in the PBS group (5.4 ± 0.5 and 9.2 ± 0.7 nmol/mg protein, respectively; $P < 0.01$; Fig. 2B), suggesting that iPSc treatment reduced lipid peroxidation and subsequent cell damage.

VASCULARIZATION AND EXPRESSION OF VEGF

To determine the mechanisms underlying the beneficial effects of iPSc transplantation, we investigated the effects of iPSc transplantation on vascularization in the post-MI hearts. At 6 weeks post-cell transplantation, immunofluorescence staining for SMA antibody indicated significant angiogenesis in iPSc-treated hearts, with more SMA-expressing vessels being present in peri-infarcted regions of the iPSc-treated hearts as compared with the PBS-treated hearts (Fig. 3A). Quantitative evaluation of the number of SMA-positive vessels per high-power field (20×) indicated that the vascular density was significantly greater in the iPSc-treated group than in

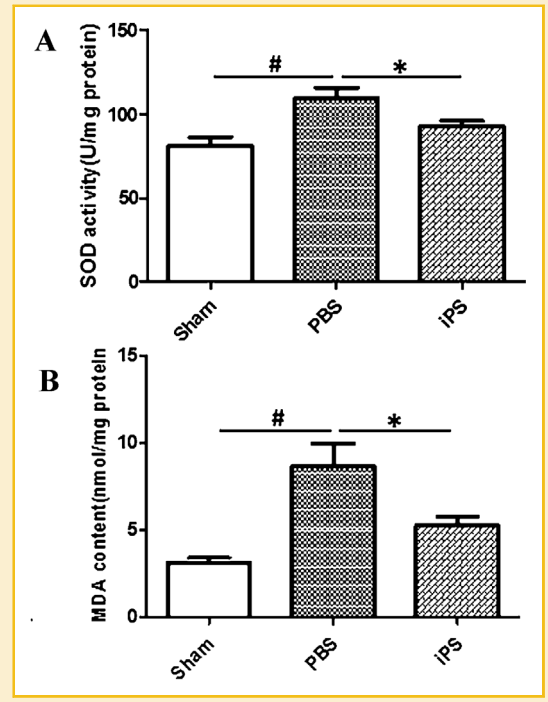

Fig. 2. iPSc treatment reduces oxidative stress. A: SOD activity in post-infarction myocardium was significantly higher in the PBS and iPS groups than in the Sham group; however, compared to the PBS group, SOD activity in the iPSc group was significantly lower. B: The malondialdehyde content of the myocardium was lower in the iPSc group than in the PBS group ($^{\#}P < 0.01$ vs. Sham, $^{*}P < 0.01$ vs. PBS).

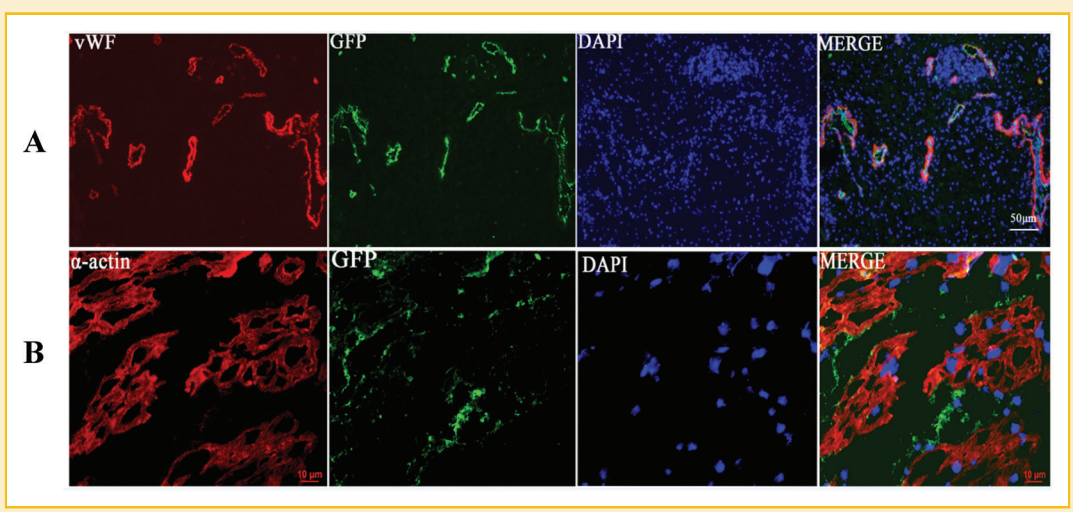

Fig. 1. The fate of engrafted iPSc cells. A: Six weeks after cell transplantation, double-label immunofluorescence staining indicated that the iPSc can survive in the BZ of infarction and have the tendency to differentiate into vascular endothelial cells. Yellow fluorescence indicates colocalization of immunofluorescent antibodies vWF (red) and GFP (green). B: Surviving iPSc were immunostained for actin with a red fluorescent marker. The lack of coexistence of GFP and actin demonstrated that there was no obvious cardiomyogenic differentiation 6 weeks after transplantation. Magnification, 200× for A, 400× for B.

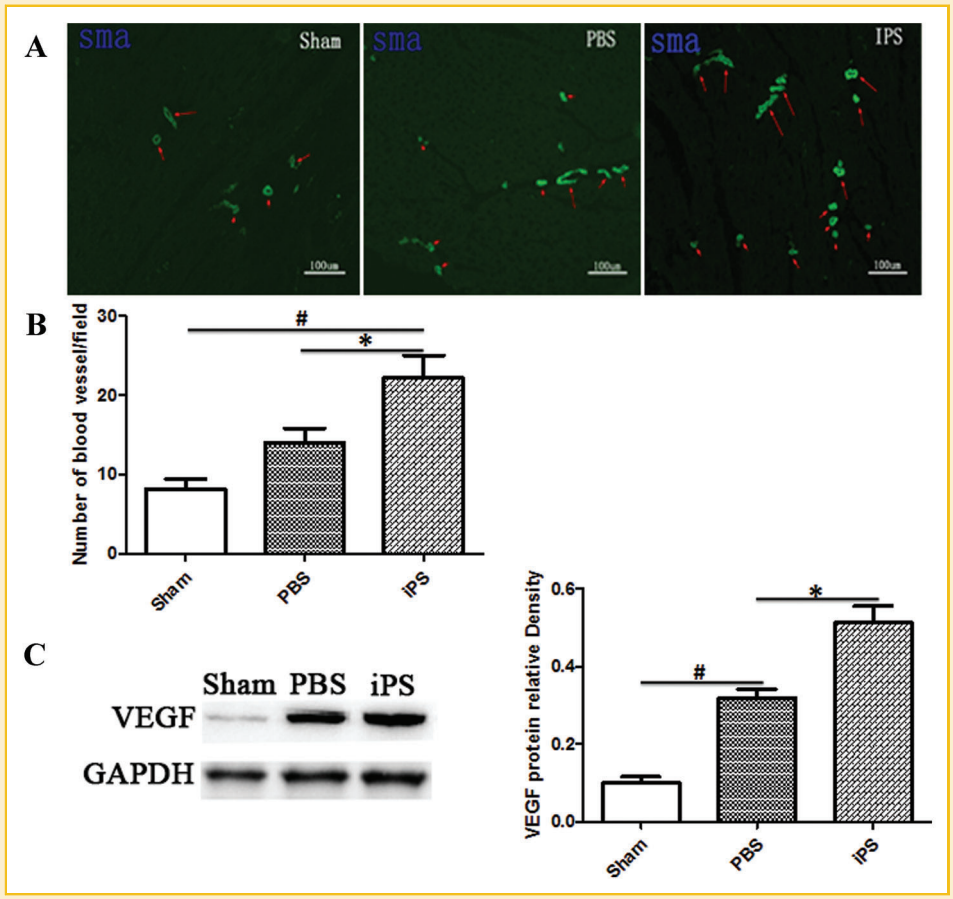

Fig. 3. Patterns of vascularization. A: The fluorescence due to SMA antibody staining demonstrated that blood vessels were increased, as shown at the red arrows. The magnification is 200×. B: Quantification of the blood vessels indicated a clear increase in the iPSc group. C and D: Western blot analysis showed a significant increase in the expression of VEGF in the iPSc group compared with the PBS group ($^{\#}P < 0.01$ vs. the Sham group; $^{*}P < 0.01$ vs. the PBS group).

the PBS-treated group (Fig. 3B). To further identify angiogenic factors, we calculated the levels of VEGF. Western blot analysis demonstrated that the expression levels of VEGF in the iPSc group were significantly higher than the PBS group at 6 weeks after cell transplantation (Fig. 3C).

AUTONOMIC NERVE SPATIAL DISTRIBUTION AND LEVELS OF ASSOCIATED PROTEINS

As revealed by immunofluorescence, the density of sympathetic nerves increased in both the PBS and iPSc groups after MI compared with the Sham group; however, in comparison with the PBS group, the sympathetic nerve density was significantly decreased and showed a more normal distribution in the iPSc group (Fig. 4A and Table I). In contrast, the density of parasympathetic nerves did not differ significantly between the groups (Fig. 4B). Consequently, it is not surprising that the iPSc transplantation significantly increased the parasympathetic/sympathetic ratio (calculated by dividing the density of parasympathetic nerves by the density of sympathetic nerves) at 6 weeks. By performing Western blotting, we found that the expression of NGF, TH, and IL-6 was significantly lower in the iPSc group than the PBS group (Fig. 4C–E). In short, iPSc administration can reduce the release of NGF and attenuate inflammatory response.

Cx43 EXPRESSION AND SPATIAL DISTRIBUTION

Immunofluorescence was performed to test Cx43 levels following iPSc transplantation. Cx43 levels in the BZ for the PBS group were dramatically reduced within the host myocardium, but partially restored by iPSc injection. The distribution of Cx43 on the BZ of post-infarcted hearts was markedly disturbed in the control group. In contrast, the disarray of Cx43 was ameliorated in the BZ of iPSc-transplanted hearts, where its distribution was relatively normal (Fig. 5A). Quantitative analysis by Western blotting showed that there was significantly less Cx43 in the BZ in the PBS group than the Sham group (Fig. 5B,C). iPSc transplantation resulted in a significant upregulation of Cx43 expression compared with PBS injection.

DYNAMIC ELECTROCARDIOGRAPHY AND VENTRICULAR PROGRAMMED ELECTRIC STIMULATION

As shown in Table II, 6 weeks after MI, we observed no major changes in the coefficient of variance and SD of the NN-interval for time domain analysis. However, the frequency domain, assessed by the LF/

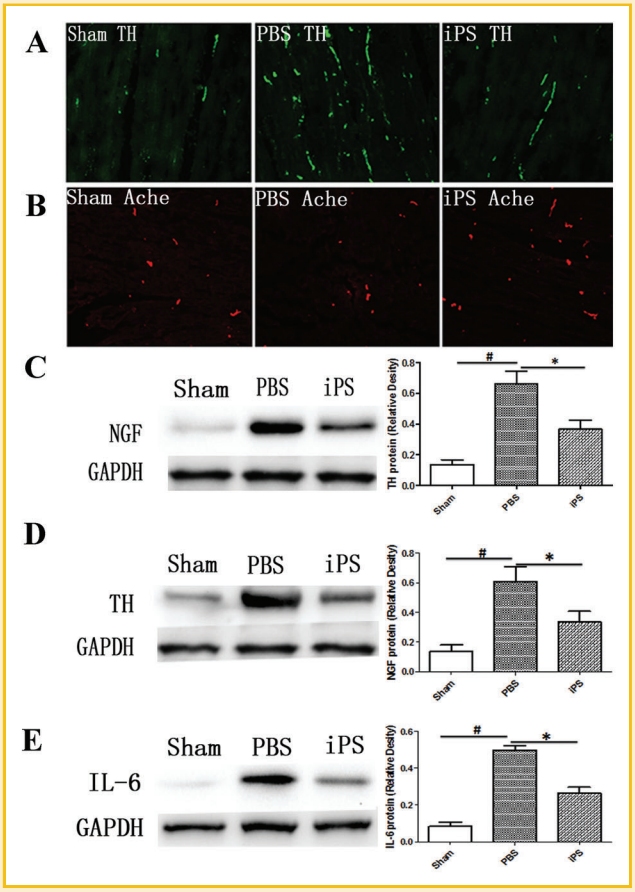

Fig. 4. Autonomic nerve spatial distribution and the level of associated proteins (A and B) sympathetic and parasympathetic nerve fibers were each stained with TH (green twigs) and Ache (red twigs) 6 weeks after MI. The nerve sprouting was observed in both experiment groups. The sympathetic sprouting in the iPSc group was reduced compared with PBS group while the parasympathetic nerve fibers had no obvious change. Accordingly, the ratio of parasympathetic to sympathetic nerves was higher in the iPSc group. Magnification, 200× for A and B. C–E: A decrease in NGF; TH and IL-6 expression was confirmed by Western blot analysis. All values were normalized to the control, which was set to 1 ($^{\#}P < 0.01$ vs. Sham, $^{*}P < 0.01$ vs. PBS); n = 6 per group.

HF ratio, was significantly decreased in the iPSc group compared with the PBS group ($P < 0.01$). A typical ECG after PES induction is shown (Fig. 6A–C). The inducibility quotient of ventricular tachycardia was significantly lower in the iPSc group versus the PBS group 6 weeks after MI (Fig. 6D).

TABLE I. Density of Nerve Fiber in the Border Zone of Infarction at 6 Weeks After Cell Transplantation

Nerve density	Sham group	PBS group	iPS group
Sympathetic ($\mu m^2/mm^2$)	$1,824 \pm 104$	$5,324 \pm 216^{*}$	$3,684 \pm 131^{\#}$
Para-sympathetic ($\mu m^2/mm^2$)	648 ± 76	$1,287 \pm 103$	$1,497 \pm 85$
Para-/sympathetic	0.35 ± 0.02	$0.23 \pm 0.02^{*}$	$0.40 \pm 0.03^{\#}$

$^{*}P < 0.05$ versus Sham group.
$^{\#}P < 0.01$ versus PBS group.

DISCUSSION

A summary of the principal findings in this study is as follows: (1) Injected iPSc survived for 6 weeks in the infarcted region and have the potential for differentiation into blood vessels; (2) Injected iPSc ameliorates neural remodeling and gap junctions remodeling; therefore, iPSc intramyocardial injection significantly inhibited the inducibility of VA.

Most previous studies have shown that only a few transplanted cells may survive in the infarction area because of the acute inflammatory response [Reinecke et al., 1999; Maurel et al., 2005; Teng et al., 2006]. However, through the use of an immunofluorescence double-staining method, our results demonstrated that myocardial-injected iPSc can persist in the infarction area and adapt to the host environment. This may be due to the use of immunity inhibitor and glucocorticoids, which can improve the local milieu in acute MI. Thus, it is reasonable to assume that such a microenvironment will allow a more effective survival and incorporation of transplanted cells. Furthermore, our results also indicated that transplanted-iPSc rarely differentiated into cardiomyocytes, but were able to differentiate into vascular endothelial cells or integrate into the growing vasculature. Our results are consistent with Davani et al. [2003] and Tomita et al. [1999], which substantiated the idea that host myocardial environment can supply the proper conditions for endothelial differentiation of stem cells and the transplanted stem cells naturally differentiate into blood vessels rather than cardiomyocytes.

Over the last several years, the research on stem cells primarily has placed an emphasis on the transformation ability in vivo and the influence of cardiac function, but has ignored the influence on the cardiac autonomic nerve system. In fact, cardiac autonomic nerve function and heart function are closely related and influence the activity of each other. In a synchronous study, another member of our group has confirmed that iPSc transplantation significantly restored cardiac function after MI [Li et al., 2013]. Herein, we focused on neural remodeling of the peri-infarct zone, which is regarded as an important component of the reentrant circuit for maintaining reentrant VA post MI [Verma et al., 2005]. Consistent with previous studies [Oh et al., 2006], our results show that sympathetic nerve sprouting at the peri-infarct zone in infarcted hearts post-MI is more excessive and heterogeneous than that in the corresponding zone in normal hearts. Compared with the PBS group, iPSc-injected hearts exhibited reduced sympathetic nerve sprouting, therefore exerting an effect of ameliorating neural remodeling.

Next, we explored the possible mechanisms of iPSc transplantation in ameliorating neural remodeling. Although the exact mechanism by which MI elicits sympathetic sprouting has not yet been clarified, it is generally accepted that NGF production is closely related with this sympathetic sprouting pathological process. Transgenic mice overexpressing NGF in the heart show cardiac hyper-innervation [Hassankhani et al., 1995], whereas the volume of the sympathetic ganglia is remarkably reduced in NGF knockout mice [Snider, 1994]. In accordance with previous studies, we also detected increased NGF protein expression in the PBS group. However, noticeably, the level of NGF expression was significantly reduced in iPSc group, thus this may partially explain the reduction of sympathetic fiber innervation.

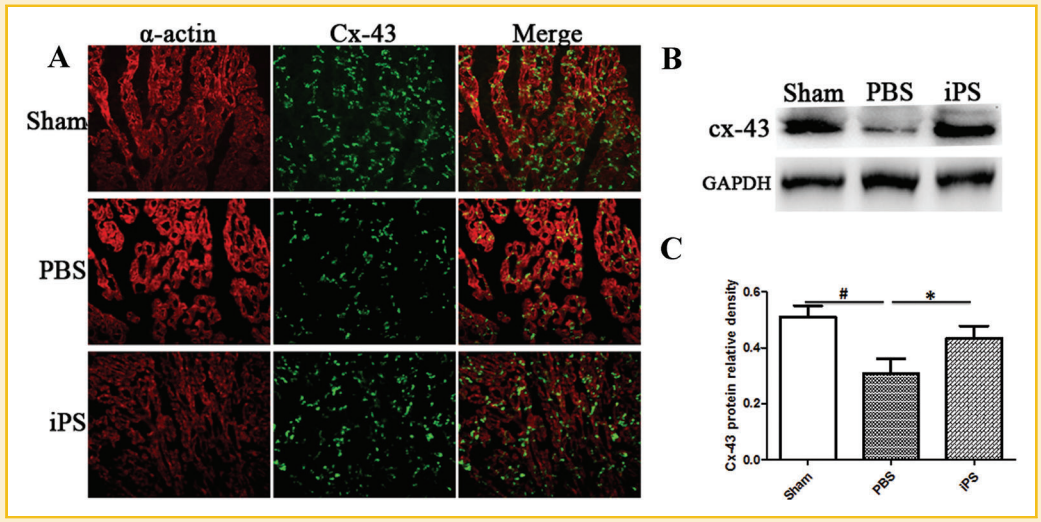

Fig. 5. Cx43 expression and spatial distribution. A: Double-label immunofluorescence show that cx43 expression in PBS-BZ showed a disturbed lateralization pattern, and was reduced, but the iPSc-BZ is similar to the Sham group. The magnification is 200×. B and C: The expression level of cx43 was confirmed by Western blot analysis. ($^{\#}P < 0.05$ vs. the Sham group; * $P < 0.05$ vs. the PBS group). There were no significant differences between the iPSc and Sham groups.

In addition, recent evidence indicates that increased oxidative damage and inflammation lead to sympathetic neural remodeling by upregulation of NGF expression [Hasan et al., 2006; Wernli et al., 2009]. Stem cell transplantation is known to suppress the release of inflammatory cytokines post-MI [Yang et al., 2008]. Here, we also detected reduced expression of IL-6 in the iPSc group. This may be related to reduce myocardial injury due to improved blood supply, as reported by previous study [Yang et al., 2008; Chen et al., 2013]. Our results also indicated that iPSc administration may inhibit the oxidative stress level in the infarcted myocardium during the chronic stage. However, a limitation in our study was that we did not study antioxidant defenses such as glutathione, so we cannot determine the exact effects of iPS transplantation on antioxidant defenses. In short, iPSc administration may reduce the release of NGF by attenuating oxidative stress and inflammatory response.

In the present study, we used dynamic electrocardiography and PES in sedated pigs to evaluate the anti-arrhythmic effects of iPSc transplantation. The ratio of LF to HF, which is an indicator of autonomic nervous activity, was decreased after iPSc transplantation.

TABLE II. Heart Rate Variability After Myocardial Infarction

	Six weeks later		
HRV	Sham group	PBS group	iPS group
Time domain			
SDNN (mm)	5.63 ± 0.47	6.79 ± 0.71	5.45 ± 1.46
CV (%)	4.54 ± 0.52	4.98 ± 0.78	3.86 ± 0.86
Frequency domain			
LF (nU)	49.30 ± 11.40	70.80 ± 14.60*	64.70 ± 7.90#
HF (nU)	29.50 ± 7.60	18.50 ± 6.20	29.50 ± 3.20
LF/HF (%)	1.67 ± 0.12	3.82 ± 0.58*	2.19 ± 0.21#

*$P < 0.05$ versus Sham group.
#$P < 0.01$ versus PBS group.

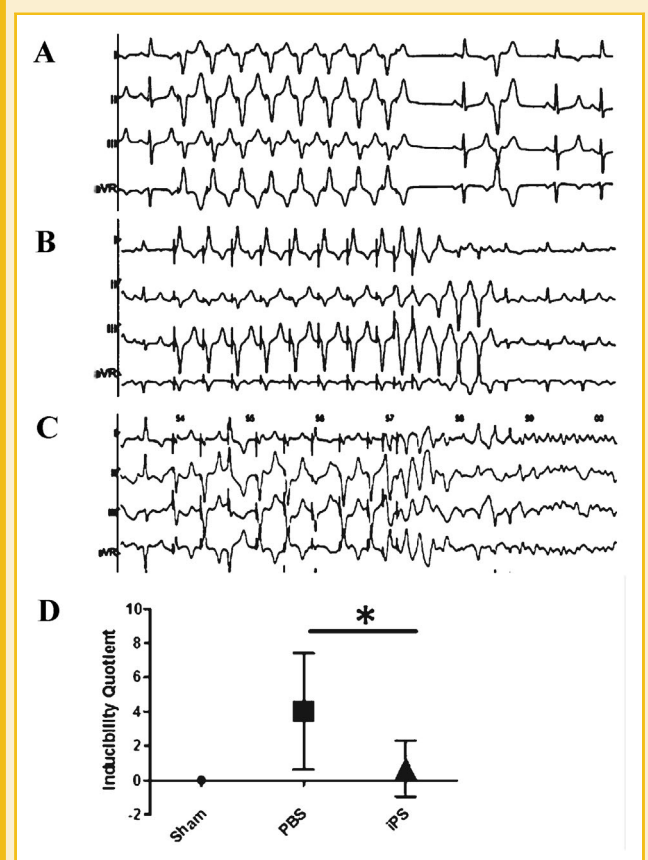

Fig. 6. Ventricular arrhythmia inducibility by programmed stimulation. Representative normal ECG (A), monomorphic ventricular tachycardia (VT) (B), and ventricular fibrillation induced by programmed stimulation using extra stimuli (C). Arrhythmia scoring shows that VA induction was less likely in iPSc-treated hearts than in PBS-treated hearts (D) ($^{*}P < 0.05$ vs. the PBS group).

Meanwhile, the susceptibility of induced VA was reduced, as assessed in the PES study. Overall, the in vivo electrophysiological study indicates that iPSc transplantation may normalize the irritable myocardium following MI. The possible mechanisms involve two aspects: (1) it is well known that regional non-heterogeneity of sympathetic innervation is closely related to electrical non-homogeneity. The enhanced spatial non-homogeneity in cardiac sympathetic innervation could amplify the spatial non-homogeneity of these electrophysiological properties and therefore facilitate the initiation of VA [Cao et al., 2000]. In this study, the inhibition of sympathetic remodeling was accompanied by the amelioration of electrical remodeling in iPSc-treated swine, indicating that iPSc may contribute to the reduction of induced VA by improving the spatial distribution of the sympathetic nerve reinnervation. (2) The remodeling of gap junctions is another pivotal event in the occurrence of VA [Wang et al., 2011]. Cardiac-restricted knockout of Cx43 causes a slowed ventricular conduction velocity and spontaneous VA in the post-infarcted hearts [Gutstein et al., 2001]. In this study, the BZ of infarction in PBS-treated hearts showed a marked disruption in gap-junction distribution, in contrast, the disarray of Cx43 was ameliorated in the BZ of iPSc-transplanted hearts, displaying a relatively normal distribution. Moreover, the myocardial Cx43 level was reduced in the PBS group and was partially restored by iPSc therapy. Thus, amelioration of Cx43 remodeling post-MI may be a shared mechanism by which iPSc transplantation contribute to the reduction of induced VA.

In summary, our research illustrated the effects of iPSc transplantation on cardiac autonomic nerve regeneration after MI. This study suggests that iPSc intramyocardial transplantation reduces vulnerability to VA, and the mechanism may be related to the remodeling of autonomic nerves and gap junctions. Taken together, our results provide useful clues for the clinical application of iPSc to prevent VAs after MI.

REFERENCES

Billman GE. 2009. Cardiac autonomic neural remodeling and susceptibility to sudden cardiac death: Effect of endurance exercise training. Am J Physiol Heart Circ Physiol 297:H1171–H1193.

Cao JM, Fishbein MC, Han JB, Lai WW, Lai AC, Wu TJ, Czer L, Wolf PL, Denton TA, Shintaku IP, Chen PS, Chen LS. 2000. Relationship between regional cardiac hyperinnervation and ventricular arrhythmia. Circulation 101:1960–1969.

Chen X, Gu M, Zhao X, Zheng X, Qin Y, You X. 2013. Deterioration of cardiac function after acute myocardial infarction is prevented by transplantation of modified endothelial progenitor cells overexpressing endothelial NO synthases. Cell Physiol Biochem 31:355–365.

Davani S, Marandin A, Mersin N, Royer B, Kantelip B, Herve P, Etievent JP, Kantelip JP. 2003. Mesenchymal progenitor cells differentiate into an endothelial phenotype, enhance vascular density, and improve heart function in a rat cellular cardiomyoplasty model. Circulation 108(Suppl1):II253–II258.

Gutstein DE, Morley GE, Tamaddon H, Vaidya D, Schneider MD, Chen J, Chien KR, Stuhlmann H, Fishman GI. 2001. Conduction slowing and sudden arrhythmic death in mice with cardiac-restricted inactivation of connexin43. Circ Res 88:333–339.

Hasan W, Jama A, Donohue T, Wernli G, Onyszchuk G, Al-Hafez B, Bilgen M, Smith PG. 2006. Sympathetic hyperinnervation and inflammatory cell NGF synthesis following myocardial infarction in rats. Brain Res 1124:142–154.

Hassankhani A, Steinhelper ME, Soonpaa MH, Katz EB, Taylor DA, Andrade-Rozental A, Factor SM, Steinberg JJ, Field LJ, Federoff HJ. 1995. Over-expression of NGF within the heart of transgenic mice causes hyperinnervation, cardiac enlargement, and hyperplasia of ectopic cells. Dev Biol 169: 309–321.

Ho YS, Magnenat JL, Bronson RT, Cao J, Gargano M, Sugawara M, Funk CD. 1997. Mice deficient in cellular glutathione peroxidase develop normally and show no increased sensitivity to hyperoxia. J Biol Chem 272:16644–16651.

Huikuri HV, Castellanos A, Myerburg RJ. 2001. Sudden death due to cardiac arrhythmias. N Engl J Med 345:1473–1482.

Kang CS, Chen CC, Lin CC, Chang NC, Lee TM. 2009. Effect of ATP-sensitive potassium channel agonists on sympathetic hyperinnervation in postinfarcted rat hearts. Am J Physiol Heart Circ Physiol 296:H1949–H1959.

Kikugawa K, Kojima T, Yamaki S, Kosugi H. 1992. Interpretation of the thiobarbituric acid reactivity of rat liver and brain homogenates in the presence of ferric ion and ethylenediaminetetraacetic acid. Anal Biochem 202:249–255.

Kruger C, Kalenka A, Haunstetter A, Schweizer M, Maier C, Ruhle U, Ehmke H, Kubler W, Haass M. 1997. Baroreflex sensitivity and heart rate variability in conscious rats with myocardial infarction. Am J Physiol 273:H2240–H2247.

Lee TM, Lin MS, Chou TF, Tsai CH, Chang NC. 2004. Adjunctive 17beta-estradiol administration reduces infarct size by altered expression of canine myocardial connexin43 protein. Cardiovasc Res 63:109–117.

Lee TM, Lin MS, Chang NC. 2007. Effect of pravastatin on sympathetic reinnervation in postinfarcted rats. Am J Physiol Heart Circ Physiol 293: H3617–H3626.

Li X, Zhang F, Song G, Gu W, Chen M, Yang B, Li D, Wang D, Cao K. 2013. Intramyocardial injection of pig pluripotent stem cells improves left ventricular function and perfusion: A study in a porcine model of acute myocardial infarction. PLoS ONE 8:e66688.

Liu YB, Wu CC, Lu LS, Su MJ, Lin CW, Lin SF, Chen LS, Fishbein MC, Chen PS, Lee YT. 2003. Sympathetic nerve sprouting, electrical remodeling, and increased vulnerability to ventricular fibrillation in hypercholesterolemic rabbits. Circ Res 92:1145–1152.

Maurel A, Azarnoush K, Sabbah L, Vignier N, Le Lorc′H M, Mandet C, Bissery A, Garcin I, Carrion C, Fiszman M, Bruneval P, Hagege A, Carpentier A, Vilquin JT, Menasche P. 2005. Can cold or heat shock improve skeletal myoblast engraftment in infarcted myocardium? Transplantation 80:660–665.

Narazaki G, Uosaki H, Teranishi M, Okita K, Kim B, Matsuoka S, Yamanaka S, Yamashita JK. 2008. Directed and systematic differentiation of cardiovascular cells from mouse induced pluripotent stem cells. Circulation 118: 498–506.

Oh YS, Jong AY, Kim DT, Li H, Wang C, Zemljic-Harpf A, Ross RS, Fishbein MC, Chen PS, Chen LS. 2006. Spatial distribution of nerve sprouting after myocardial infarction in mice. Heart Rhythm 3:728–736.

Reinecke H, Zhang M, Bartosek T, Murry CE. 1999. Survival, integration, and differentiation of cardiomyocyte grafts: A study in normal and injured rat hearts. Circulation 100:193–202.

Seki T, Yuasa S, Oda M, Egashira T, Yae K, Kusumoto D, Nakata H, Tohyama S, Hashimoto H, Kodaira M, Okada Y, Seimiya H, Fusaki N, Hasegawa M, Fukuda K. 2010. Generation of induced pluripotent stem cells from human terminally differentiated circulating T cells. Cell Stem Cell 7:11–14.

Snider WD. 1994. Functions of the neurotrophins during nervous system development: What the knockouts are teaching us. Cell 77:627–638.

Takahashi K, Yamanaka S. 2006. Induction of pluripotent stem cells from mouse embryonic and adult fibroblast cultures by defined factors. Cell 126:663–676.

Teng CJ, Luo J, Chiu RC, Shum-Tim D. 2006. Massive mechanical loss of microspheres with direct intramyocardial injection in the beating heart: implications for cellular cardiomyoplasty. J Thorac Cardiovasc Surg 132: 628–632.

Tomita S, Li RK, Weisel RD, Mickle DA, Kim EJ, Sakai T, Jia ZQ. 1999. Autologous transplantation of bone marrow cells improves damaged heart function. Circulation 100:II247–II256.

Verma A, Marrouche NF, Schweikert RA, Saliba W, Wazni O, Cummings J, Abdul-Karim A, Bhargava M, Burkhardt JD, Kilicaslan F, Martin DO, Natale A. 2005. Relationship between successful ablation sites and the scar border zone defined by substrate mapping for ventricular tachycardia post-myocardial infarction. J Cardiovasc Electrophysiol 16:465–471.

Wang D, Zhang F, Shen W, Chen M, Yang B, Zhang Y, Cao K. 2011. Mesenchymal stem cell injection ameliorates the inducibility of ventricular arrhythmias after myocardial infarction in rats. Int J Cardiol 152:314–320.

Wernli G, Hasan W, Bhattacherjee A, van Rooijen N, Smith PG. 2009. Macrophage depletion suppresses sympathetic hyperinnervation following myocardial infarction. Basic Res Cardiol 104:681–693.

Wu Z, Chen J, Ren J, Bao L, Liao J, Cui C, Rao L, Li H, Gu Y, Dai H, Zhu H, Teng X, Cheng L, Xiao L. 2009. Generation of pig induced pluripotent stem cells with a drug-inducible system. J Mol Cell Biol 1:46–54.

Yang YJ, Qian HY, Huang J, Geng YJ, Gao RL, Dou KF, Yang GS, Li JJ, Shen R, He ZX, Lu MJ, Zhao SH. 2008. Atorvastatin treatment improves survival and effects of implanted mesenchymal stem cells in post-infarct swine hearts. Eur Heart J 29:1578–1590.

Zhang S, Ge J, Zhao L, Qian J, Huang Z, Shen L, Sun A, Wang K, Zou Y. 2007. Host vascular niche contributes to myocardial repair induced by intracoronary transplantation of bone marrow CD34+ progenitor cells in infarcted swine heart. Stem Cells 25:1195–1203.

Zeng L, Hu Q, Wang X, Mansoor A, Lee J, Feygin J, Zhang G, Suntharalingam P, Boozer S, Mhashilkar A, Panetta CJ, Swingen C, Deans R, From AH, Bache RJ, Verfaillie CM, Zhang J. 2007. Bioenergetic and functional consequences of bone marrow-derived multipotent progenitor cell transplantation in hearts with postinfarction left ventricular remodeling. Circulation 115: 1866–1875.

SUPPORTING INFORMATION

Additional supporting information may be found in the online version of this article at the publisher's web-site.